Controlling the composition, microstructure, electrical and magnetic properties of LiFe5O8 powders…

Article *in* Journal of Magnetism and Magnetic Materials · January 2015

DOI: 10.1016/j.jmmm.2014.08.090

CITATIONS
5

READS
45

5 authors, including:

Mohamed M Rashad
Central Metallurgical Research and Develop…
149 PUBLICATIONS **1,990** CITATIONS
SEE PROFILE

M. G. El-Shaarawy
Benha University
36 PUBLICATIONS **277** CITATIONS
SEE PROFILE

N. M. Shash
Benha University
32 PUBLICATIONS **108** CITATIONS
SEE PROFILE

Journal of Magnetism and Magnetic Materials 374 (2015) 495–501

Contents lists available at ScienceDirect

Journal of Magnetism and Magnetic Materials

journal homepage: www.elsevier.com/locate/jmmm

Controlling the composition, microstructure, electrical and magnetic properties of $LiFe_5O_8$ powders synthesized by sol gel auto-combustion method using urea as a fuel

M.M. Rashad [a,*], M.G. El-Shaarawy [b], N.M. Shash [b], M.H. Maklad [b], F.A. Afifi [c]

[a] Central Metallurgical Research and Development Institute (CMRDI), Helwan, Cairo, Egypt
[b] Physics Department, Benha University, Benha, Egypt
[c] Basic Engineering Science Department, Faculty of Engineering, Benha university, Benha, Egypt

ARTICLE INFO

Article history:
Received 20 July 2014
Received in revised form
13 August 2014
Available online 1 September 2014

Keywords:
Spinel ferrite
Combustion synthesis
Microstructure
Electrical property
Magnetic property

ABSTRACT

Nanocrystalline lithium ferrite $LiFe_5O_8$ powders were synthesized by the sol gel auto-combustion method from the corresponding metal nitrates using urea as a fuel. DTA results showed that the $LiFe_5O_8$ phase started to form at temperature around 385 °C. X-ray diffraction analysis indicates that all compositions were formed in a single-phase cubic spinel structure at different annealing temperatures from 400 to 800 °C for 2 h. The lattice parameter was found to decrease whereas the particle size was increased with annealing temperature. The frequency exponent "*s*" of lithium ferrite lies in the range $0.5 \leq s \leq 1$, which confirmed the electron hopping between Fe^{2+} and Fe^{3+} ions. The electron mobility in $LiFe_5O_8$ samples ranged from 0.05 to 0.29 eV, which clearly indicated that the present lithium ferrites have semiconductor-like behavior. The saturation magnetization was increased on increasing the annealing temperature up to 800 °C. High saturation magnetization ($Ms = 51.9$ emu/g) was achieved for the ferrite powders produced at annealing temperature 800 °C for 2 h.

1. Introduction

Lithium ferrite $LiFe_5O_8$ has drawn attention from a long time due to its unique excellent properties such as high saturation magnetization, low dielectric losses, excellent square shape of hysteresis curve, excellent dielectric properties, high Curie temperature (620 °C), high chemical inertness, thermal stability, high resistivity, low eddy current losses, low cost and safety. Due to these desirable properties, it is widely used in prolonged technological applications such as lithium ion batteries, high-density magnetic recording, magnetic fluids, magneto-caloric refrigeration, magnetic resonance imaging enhancement, and magnetically guided drug delivery and is very attractive as a substitute for expensive yttrium iron garnet (YIG) in mass-scale microwave devices such as circulators, phase shifters, isolators, power transformation in electronics, memory core, antennas and high-speed digital tapes [1–4]. Thus, it is important to obtain lithium ferrite of high purity using an easy preparation method. The solid-state method (solid reaction mixtures of oxides annealed at high temperature) as the most employed method suffers from the evaporation of Li ions during processing, which affects the properties of the resultant products due to the formation of secondary iron oxide phase [5]. Thus, to achieve highly homogeneous lithium ferrite particles, numerous wet chemical methods have been applied to synthesize lithium ferrite fine particles including ball milling [6], sol gel [7], combustion method [8–9], solvothermal [10], hydrothermal [11], aerosol route [12] co-precipitation [13–14] and microemulsion [14] techniques. Recently, combustion synthesis has emerged as an attractive technique for the excellent chemical homogeneity, high purity and crystalline spinel powders. Moreover, this method has been adopted due to its many advantages compared with other methods such as energy efficiency, short reaction rate, nano-sized powders, the reagents are simple compounds, easy operable, dopants can be easily introduced into the final product, low annealing temperature due to use of the energy produced by the exothermic decomposition of a redox mixture of metal nitrates with an organic compound, better particle size distribution, high probability of formation of single domain and agglomeration of powders remains limited [15–19]. Thus, the present work reports the synthesis of lithium ferrite nanoparticles at different annealing temperatures synthesized through the sol–gel auto-combustion method using urea as the chelating agent and as a fuel. The effect of annealing temperature variation on structural morphology and magnetic properties of synthesized nanoparticles has been

* Corresponding author.
E-mail address: rashad133@yahoo.com (M.M. Rashad).

http://dx.doi.org/10.1016/j.jmmm.2014.08.090
0304-8853/

also investigated. The synthesized nanoparticles were characterized by TGA, DTA, XRD, EE-SEM, LCR meter and VSM to explore the temperature-dependent changes in structural morphology, electrical and magnetic properties.

2. Experimental

The organic precursor method was applied for the preparation of lithium ferrite ($LiFe_5O_8$). Chemical grade ferric nitrate $FeNO_3 \cdot 9H_2O$ (Alfa Aesar, purity 98%), lithium nitrate $LiNO_3 \cdot 3H_2O$ (Alfa Aesar, purity 98%) and urea NH_2CONH_2 (ADWIC, 98%) were used as starting materials. The mixture of lithium nitrate and ferric nitrate solution with optimum Fe^{3+}/Li^{+} molar ratio 3.33 (i.e. 5.0:1.5) to attain lithium ferrite [8] was first prepared and then stirred for 15 min on a hot-plate magnetic stirrer, followed by the addition of an aqueous solution of urea to the mixtures with stirring. The solution was evaporated to 80 °C with constant stirring and then dried in a dryer at 100 °C overnight. The dried powders were obtained as lithium ferrite precursors. Differential thermal analyzer (DTA) analysis of un-annealed precursor was carried out using NETZSCH STA 409C/CD. The rate of heating was kept at 10 °C/min between 25 and 1000 °C. The measurements were carried out in a current of argon atmosphere.

For the formation of the lithium ferrite phase, the dry precursors were annealed at the rate of 10 °C/min in static air atmosphere up to different temperatures from 300 to 800 °C and maintained at the temperature for annealed time (2 h). The crystalline phases presented in the different annealed samples were identified by XRD on a Bruker axis D8 diffractometer using Cu-Kα ($\lambda = 1.5406$) radiation and secondary monochromator in the range 2θ from 20 to 70°. The ferrite particle's morphologies were observed by a field emission scanning electron microscope (FE-SEM, QUANTA FEG 250). The ac electrical conductivity for the investigated samples was performed over a temperature range from 30 to 200 °C and frequency range from 20 Hz to 10 MHz using (LCR-8110G) precision LCR meter. The magnetic properties of the ferrites were measured at room temperature using a vibrating sample magnetometer (VSM; 9600-1 LDJ, USA) in a maximum applied field of 15 kOe. From the obtained hysteresis loops, the saturation magnetization (M_s), remanence magnetization (M_r) and coercivity (H_c) were determined.

3. Results and discussion

3.1. Thermal analysis

Fig. 1 shows the thermal analysis of unannealed lithium ferrite precursor synthesized at Fe^{3+}/Li^{+} molar ratio 3.33 (i.e. 5.0:1.5) using urea as a fuel and a chelating agent. The results illustrate that the lithium iron urea precursor decomposed thermally in two endothermic steps. The first endothermic step started at 57.8–228.2 °C due to loss of physically and chemically sorbed/bonded water and decomposition of urea to evolve CO_2, H_2O and NO_2 gases. After dehydration reaction, the anhydrous ferrite precursor was decomposed into Li_2O and Fe_2O_3. The second endothermic step started at 384.5 °C and it is related to the solid–solid interaction of Li_2O and Fe_2O_3 to form nanocrystalline lithium ferrite powders. This indicates that the decomposition of the gels occurred suddenly in a single step, as observed in other systems [8]. From TGA data of the lithium ferrite dried gel powder, the weight loss profile shows two weight loss regions, the first weight loss (~16%) region beginning from 57.8 °C to maximum 228.2 °C corresponded to the removal of water chemical bonds and decomposition of nitrate group and urea with the evolution of great amounts of gases. The second endothermic weight loss (~7%) occurred in the range of 384.5–400 °C and was attributed

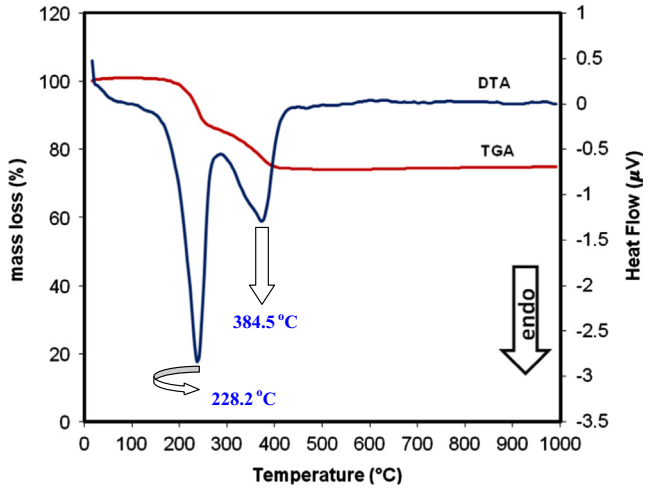

Fig. 1. Thermal analysis profiles of un-annealed lithium ferrite precursor.

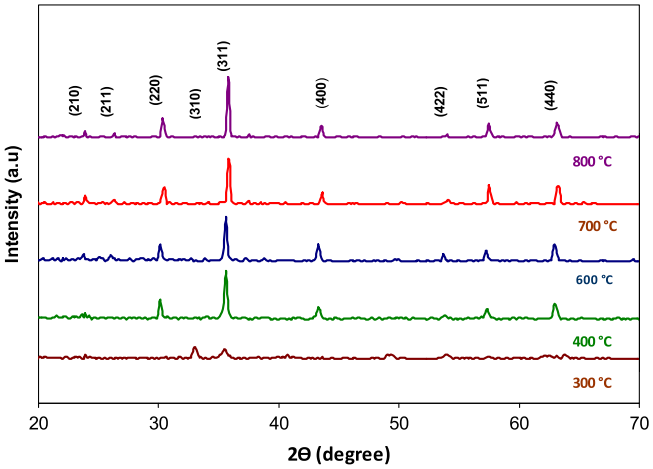

Fig. 2. XRD patterns of lithium ferrite precursors synthesized annealed at different temperatures from 300 to 800 °C for 2 h.

to the transformation of Li_2O and Fe_2O_3 to spinel ferrite. No significant weight loss was observed above 400 °C, indicating that the precursor generates a stable phase after the heat-treatment at temperature above 400 °C. In this case, nanosized lithium ferrite can be obtained at much lower temperature compared with conventional ceramic method and the previous published lithium ferrite using citrate and oxalate precursor routes.

3.2. Crystal structure

Fig. 2 evidences the powder X-ray diffraction patterns of lithium ferrite powders synthesized by sol–gel auto-combustion using urea annealed at different temperatures from 300 to 800 °C for 2 h. For the sample treated at 300 °C, the pattern was extremely broad and it had amorphous structure, indicating that the ferrite particles formed are extremely small. The peak (310) matched for the sample annealed at 300 °C was related to the $LiFeO_2$ phase. The diffraction patterns of the samples annealed at different temperatures from 400 to 800 °C exhibited good crystalline cubic $LiFe_5O_8$ (JCPDS # 82-1436) phase. The diffraction peaks corresponding to (210) (211) (220) (311) (400) (422) (511) and (400) planes of lithium spinel ferrite were ascribed. It is also noticed from Fig. 2 that all the peaks have the same fixed position with small shift to high 2θ and the crystallinity of the produced ferrite powders was found to increase with increasing annealing temperatures from 400 to 800 °C. This means that a gradual increase in crystallite size as a function of heat treatment temperature

Table 1
Average crystallite size, lattice parameter and unit cell volume of all samples annealed at different temperatures from 300 to 800 °C for 2 h.

Annealing temp (°C)	Average crystallite size (nm)	Lattice constant a (Å)	Cell volume V (Å³)
300	–	–	–
400	49.46	8.34	580.09
600	55.15	8.33	578.01
700	68.83	8.32	575.93
800	91.48	8.31	573.85

is expected as given in Table 1. The crystallite sizes of the produced cobalt ferrites for the most intense peak [(311) plane] observed at $2\theta \approx 35.825^{\circ}$ were calculated from the XRD data based on the Debye–Scherrer formula. It was found to increase from 49.5 nm at 400 °C to 91.5 nm at 800 °C. Lattice parameter (a) as well as unit cell volume (V_{cell}) of the lithium ferrite specimens was calculated and the results are listed in Table 1. The measured lattice parameter for $LiFe_5O_8$ phase was found to be 0.833 ± 0.01 nm, which is in good agreement with that mentioned in the ICDD card.

3.3. Microstructure

Magnetic and electrical properties sensitively depended on the microstructure of ferrites. Between grain size and porosity of microstructures, grain size is the more important parameter affecting the magnetic properties of ferrites. Grain growth is closely related to the grain boundary mobility [1]. Fig. 3 presents the field emission scanning electron microscope (FE-SEM) of $LiFe_5O_8$ powders synthesized from the lithium–iron precursor with Fe^{3+}/L^{i+} mole ratio 3.33 thermally treated at different temperatures (300, 400, 600,700 and 800 °C) for 2 h. As shown in Fig. 3, increase in the grain size with the heat treatment temperatures was observed. The sample heat-treated at 300 °C exhibits small grains with a quasi-spherical shape with irregular microstructures indicating that the composition is insufficient for the complete formation of the structure. The spherical geometrical definition with uniform structure and a well-clear crystalline microstructure increases for the sample treated at 400 °C due to the formation of the lithium ferrite phase. The average grain sizes were ~40 and 75 nm for the samples produced at annealing temperatures of 300 and 400 °C, respectively. As can be seen, the grain growth was enhanced as the annealing temperature was raised up to 600 and 700 °C. The average particle sizes were 140 and 175 nm, respectively. Moreover, the grain patterns exhibited spherical-like structure. As the annealing temperature increased to 800 °C, a clear crystalline structure was observed. The SEM micrographs suggest that the thermal treatment at 800 °C promotes the aggregation of those spherical grains with the largest size. Furthermore, it seems that the structure that was observed in the sample treated at lower temperature was grown in many directions to give a quasi-octahedral honey network-like structure at 800 °C. Furthermore, it was found that lithium ferrite powder granules were made up of overall crystallite aggregates (200–500 nm).

3.4. Electrical properties

3.4.1. The temperature dependence of ac conductivity

The temperature dependence of ac conductivity, σ_{ac}, for all investigated samples using urea annealed at different temperatures has been studied in the temperature range 30–200 °C and frequency range from 20 Hz to 10 MHz. The Arrhenius expression has been used to fit the temperature dependence of the ac conductivity, σ_{ac},

$$\sigma_{ac} = \sigma_o \exp(-E_{a(ac)}/kT) \quad (1)$$

where σ_o is the pre-exponential factor containing several constants, k is Boltzmann's constant, T is the absolute temperature and $E_{a(ac)}$ is the ac activation energy for conduction. Fig. 4 depicts the dependence of ac conductivity on the temperature for all $LiFe_5O_8$ samples annealed at different temperatures from 300 to 800 °C for 2 h on varying the frequency range from 20 Hz to 10 MHz. The activation energies are calculated from a straight line fit using Eq. (1) compositions and are given in Table 2. The data show that the ac conductivity σ_{ac} increases with the increasing of annealing temperature. This behavior can be also explained by the decrease of the hematite phase and the inclusion of the ferrite phase for the highest treatment temperatures. Furthermore, the observed behavior clearly indicates that the present lithium ferrites have a semiconductor-like behavior. The increase of electrical conductivity with increasing temperature and frequency may be related to the increase of the drift mobility of electron and hole by hopping conduction [20–21].

3.4.2. The frequency dependence of ac conductivity

Fig. 5 shows the variation of log ac electrical conductivity $\sigma_{ac}(\omega)$ with log frequency. The change in the electrical conductivity in ferrite is mainly due to the hopping of electron between ions of the same element present in more than one valance state, distributed randomly over crystallo-graphically equivalent lattice sites. Ferrites structurally form cubic close-packed oxygen lattice, with cations at octahedral (B) and tetrahedral (A) sites. The distance between two metal ions on (B) sites is smaller than the distance between two metals ions on (B) and (A) sites; therefore the hopping between (A) and (B) has very small probability compared with that for B–B hopping. The hopping between A and A sites does not exist, due to that there are only Fe^{3+} ions at A sites and any Fe^{2+} ions formed during processing preferentially occupy B-sites only. The charges can migrate under the influence of the applied field contributing to the electrical response of the system. It has been found that conductivity is an increasing function of frequency in the case of conduction by hopping and a decreasing function of frequency in case of band conduction [22]. Generally, the total conductivity obeys the following power relation:

$$\sigma_{ac}(\omega) = A\omega^s \quad (2)$$

where A is a temperature-dependent parameter, ω is the angular frequency and the frequency exponent s is a temperature-dependent parameter with values between 0.0 and 1. It can be seen that the values of conductivity gradually increase on increasing the applied field frequency. The increase in (σ_{ac}) with applied field frequency can be explained on the basis that the pumping force of the applied frequency that helps in transferring the charge carriers between the different localized states as well as liberating the trapped charges from the different trapping centers. These charge carriers participate in the conduction process simultaneously with electrons produced from the valence exchange between the different metal ions. The exponent s can be calculated as a function of composition for each sample, in the temperature range from 30 to 200 °C by plotting $\ln\sigma$ versus $\ln\omega$ according to Eq. 2 as shown in Fig. 5, which represents straight lines with slope equal to the exponent s and the variation of the exponent s is listed in Table 3. It is clear that the value of s ranges between 0 and 1. When $s=0$, the electrical conduction is frequency independent or dc conduction, but for $s \leq 1$, the conduction is frequency dependent or ac conduction. It may be noted that the exponent s lies in two ranges. In the range $0.5 \leq s \leq 1$ which confirms the electron hopping between Fe^{2+} and Fe^{3+} ions and the values of $s \leq 0.5$ which confirm the domination of ionic conductivity [23]. Therefore, the behavior of σ' with frequency and exponent s with temperature, respectively, suggests that the classical barrier hopping model is the most favorable

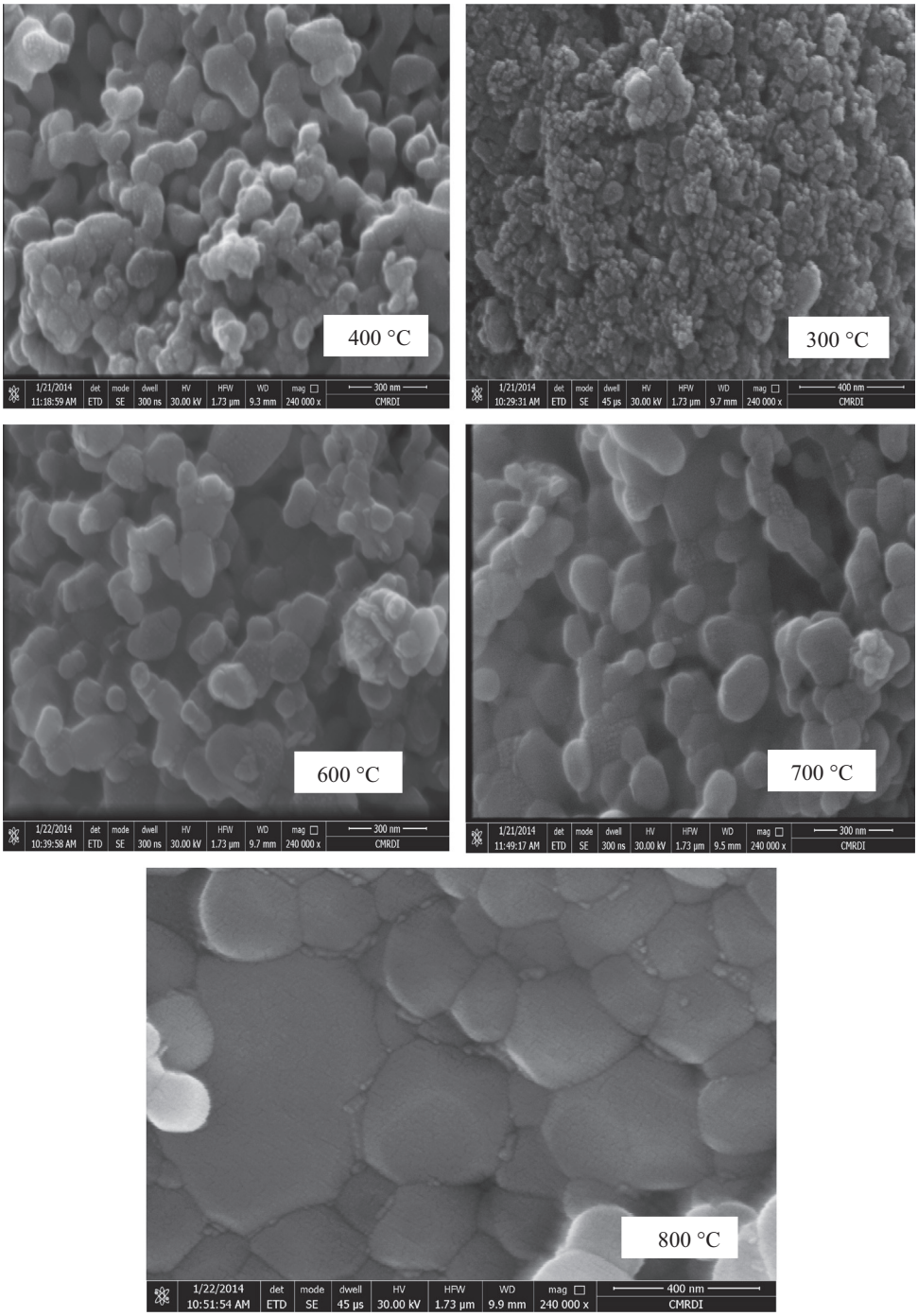

Fig. 3. FE-SEM images of the synthesized $LiFe_5O_8$ powders annealed at different temperatures from 300 to 800 °C for 2 h.

mechanism to describe the conduction mechanism for the compositions under investigation. The charge carriers responsible for the conduction process are the electron hopping between Fe^{2+} and Fe^{3+} ions in the case of Li-ferrite samples. The values of the exponent *s* are listed in Table 3. It may be noted that the exponent *s* lies in two ranges. In the range $0.5 \leq s \leq 1$ which confirms the electron hopping between Fe^{2+} and Fe^{3+} ions and the values of $s \leq 0.5$ which confirm the domination of ionic conductivity [24].

3.5. The magnetic properties

The magnetization of the produced lithium ferrite powders was performed at room temperature under an applied field of 20 kOe and the hysteresis loops of the ferrite powders were obtained. Plots of magnetization (*M*) as a function of applied field (*H*) for all lithium ferrite samples are shown in Fig. 6. From the obtained hysteresis loops, the saturation magnetization (*Ms*), remanence magnetization (*Mr*) and coercivity (*Hc*) are listed in Table 4.

Fig. 6 indicates that the lithium ferrite was a soft magnetic material due to the deviation from rectangular form and there was very low coercivity and the magnetic properties of the prepared lithium ferrites were strongly dependent on the annealing temperature. The saturation magnetization was increased steadily on increasing the annealing temperature from 400 to 800 °C. The lithium ferrite powder annealed at 800 °C for 2 h exhibited the highest saturation magnetization 51.9 emu/g. The value is higher than that obtained by

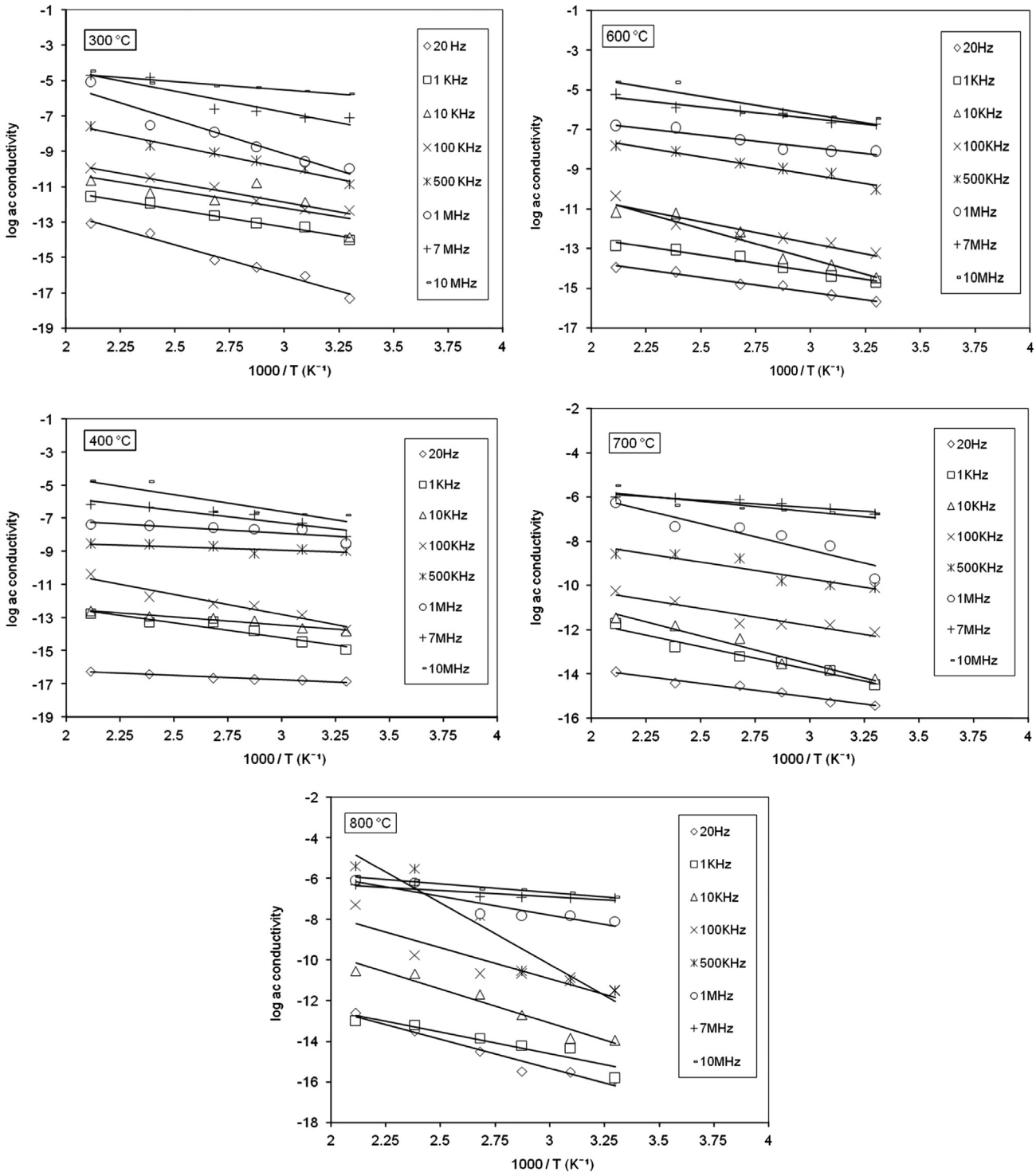

Fig. 4. Electrical conductivity versus inverse of temperatures for $LiFe_5O_8$ ferrite samples annealed for 2 h with different frequencies.

Table 2
Activation energies obtained from Arrhenius plots of the produced lithium ferrite samples annealed at different temperatures from 300 to 800 °C for 2 h.

Annealing temp (°C)	$E_{a(ac)}$ (eV)							
	20 Hz	1 KHz	10 KHz	100 KHz	500 KHz	1 MHz	7 MHz	10 MHz
300	0.300	0.172	0.168	0.189	0.215	0.330	0.203	0.082
400	0.045	0.154	0.085	0.208	0.037	0.064	0.131	0.176
600	0.129	0.142	0.265	0.188	0.153	0.109	0.102	0.156
700	0.108	0.179	0.218	0.135	0.131	0.205	0.058	0.081
800	0.246	0.183	0.286	0.264	0.521	0.160	0.054	0.073

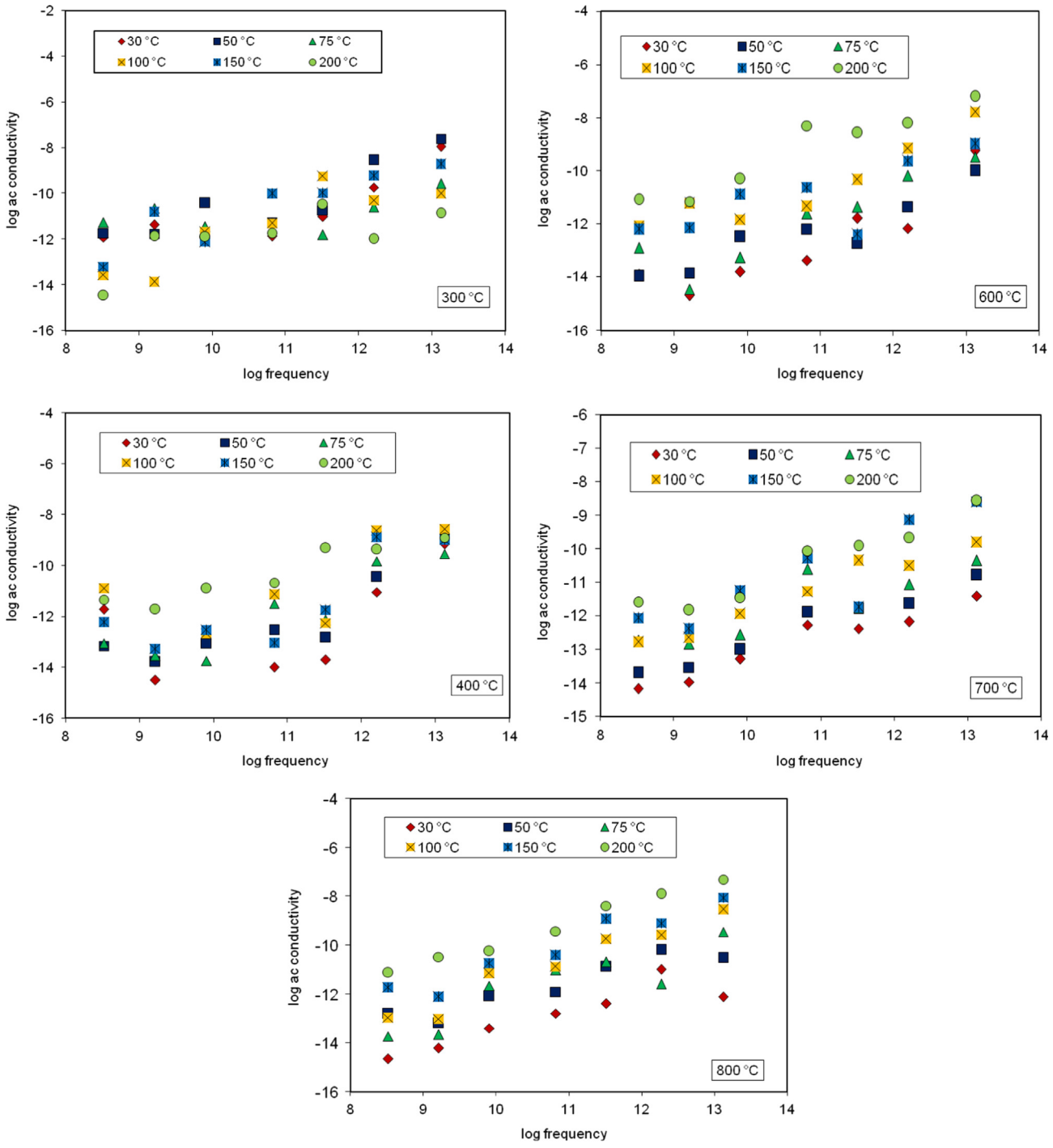

Fig. 5. Dependence of ac conductivity on the frequency for all $LiFe_5O_8$ samples annealed at different temperatures for 2 h.

Table 3
The values of the exponent "*s* value" for the produced lithium ferrite samples annealed at different temperatures from 300 to 800 °C for 2 h.

Annealing temp. (°C)	*S*-value					
	30 °C	50 °C	75 °C	100 °C	150 °C	200 °C
300	0.757	0.861	0.233	0.940	0.879	0.555
400	0.653	0.970	0.923	0.790	0.892	0.636
600	0.994	0.777	0.974	0.868	0.612	0.906
700	0.603	0.647	0.547	0.696	0.770	0.702
800	0.692	0.648	0.831	0.998	0.874	0.855

Cheruku et al. [25] in which the saturation magnetization was 43.44 emu/g for the pure lithium ferrite synthesized by solution combustion using citric acid as an organic fuel annealed at 900 °C for 6 h. However, the value is lower than the value ($Ms = 68.7$ emu/g) obtained by Hessien [8] for the lithium ferrite powders prepared at annealing temperature 1000 °C for 2 h using oxalic acid as organic fuel and oxidizing agent as the results of the increasing of the crystallite size (120.2 nm) compared by our sample with crystallite size (91.5 nm). Singhal et al. [26] indicated that the saturation magnetization of $LiFe_5O_8$ ferrite was organic fuel dependent. The saturation magnetization was 59.5, 55.9 and 50.2 emu/g for the

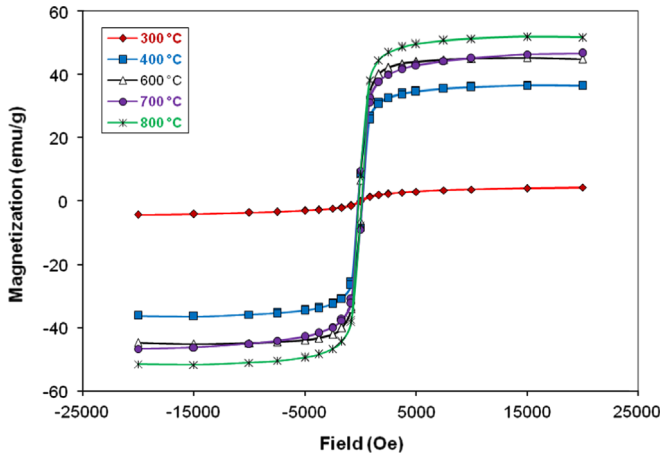

Fig. 6. *M–H* hysteresis loop of all lithium ferrite samples annealed at different temperatures from 300 to 800 °C for 2 h.

Table 4
The magnetic properties for the produced lithium ferrite samples annealed at different temperatures from 300 to 800 °C for 2 h.

Annealing temp (°C)	*Ms* (emu/g)	*Mr* (emu/g)	*Hc* (Oe)
300	4.30	0.22	120.52
400	36.55	8.44	198.01
600	45.24	6.37	133.41
700	46.67	9.36	193.05
800	51.90	7.96	145.72

produced ferrite sample at annealing temperature 1000 °C for 2 h with Li/Fe molar ratio 1:5 using citric acid, glycine and urea, respectively. The increase in the saturation magnetization by increasing the annealing temperature was due to the increase in phase purity and well-defined crystallinity of $LiFe_5O_8$. The crystallite size increased from 49.5 nm for the samples annealed at 400 °C to 91.5 nm for the samples annealed at 800 °C. There was a fall in saturation magnetization of the sample annealed at 300 °C as a result of amorphous structure and the presence of non-magnetic elements as confirmed by XRD analysis. The coercive force H_c of the formed lithium ferrite ranged from 120 to 206 Oe depending on the annealing temperature. The smaller values of coercivity (less than 200 Oe) might be due to the single domain behavior, suggesting that the particle size in these compounds is less than a critical value, which is usually taken about few hundred angstroms [5].

4. Conclusions

In monitoring the conditions of the synthesis method, lithium ferrite powders have been successfully synthesized by the sol gel auto-combustion method using urea as an organic fuel. The results from DTA, XRD, SEM, AC electrical conductivity and VSM studies are summarized as follows:

- By thermal analysis, it was proved that the precursors were decomposed into lithium ferrite phase at 385 °C.
- The results of XRD analysis showed that all the samples were formed in single-phase cubic spinel structure at different annealing temperatures from 400 to 800 °C for 2 h. The lattice parameter was found to decrease on increasing the temperature
- The microstructure of lithium ferrite powders was temperature dependent. The particle size was increased with the annealing temperature.
- AC electrical properties were investigated using the super-linear power law and activation energies were calculated for all compositions. The electron mobility in $LiFe_5O_8$ samples ranged from 0.05 to 0.29 eV, which clearly indicated that the present lithium ferrites have semiconductor-like behavior.
- The frequency exponent "*s*" of lithium ferrite lies in the range $0.5 \leq s \leq 1$, which confirms the electron hopping between Fe^{2+} and Fe^{3+} ions.
- The formed crystalline pure lithium ferrite powders had good magnetic properties. High saturation magnetization ($Ms = 51.9$ emu/g) was achieved for the formed lithium ferrite phase at annealing temperature 800 °C for 2 h.

Acknowledgments

This research was financially supported by the Central Metallurgical Research and Development Institute, Egypt, Grant no. Project ID 983.

References

[1] S.A. Mazen, N.I. Abu-Elsaad, Ceram. Int. 40 (2014) 11229.
[2] M. Srivastava, S. Layek, J. Singh, A.K. Das, H.C. Verma, A.K. Ojha, N.H. Kim, J.H. Lee, J. Alloys Compd. 591 (2014) 174.
[3] V. Mohanty, R. Cheruku, L. Vijayan, G. Govindaraj, J. Mater. Sci. Technol. 30 (2014) 335.
[4] S.S. Teixeira, M.P.F. Graça, L.C. Costa, J. Non-Cryst. Solids 358 (2012) 1924.
[5] P.R. Arjunwadkar, R.R. Patil, J. Alloys Compd. 611 (2014) 273.
[6] S.S. Teixeira, M.P.F. Graça, L.C. Costa, M.A. Valente, Mater. Sci. Eng.: B 186 (2014) 83.
[7] M. Srivastava, A.K. Ojha, S. Chaubey, P.K. Sharma, A.C. Pandey, Mater. Sci. Eng.: B 175 (2010) 14.
[8] M.M. Hessien, J. Magn. Magn. Mater. 320 (2008) 2800.
[9] P.P. Hankare, R.P. Patil, U.B. Sankpal, K.M. Garadkar, R. Sasikala, A.K. Tripathi, I.S. Mulla, J. Magn. Magn. Mater. 322 (2010) 2629.
[10] B. Li, Y. Xie, H. Su, Y. Qian, X. Liu, Solid State Ion. 120 (1999) 251.
[11] H. Zeng, T. Tao, Y. Wu, W. Qi, C. Kuang, S. Zhouand, Y. Chen, RSC Adv. 4 (2014) 23145.
[12] S. Singhal, K. Chandra, J. Electromagn. Appl. Anal. 2 (2010) 51.
[13] C. Barriga, V. Barron, R. Gancedo, M. Gracia, J. Morales, J.L. Tirado, J. Torrent J. Solid State Chem. 77 (1988) 132.
[14] M. Abdullah Dar, Jyoti Shah, W.A. Siddiqui, R.K. Kotnala, J. Alloys Compd. 523 (2012) 36.
[15] R.M. Mohamed, M.M. Rashad, F. Harraz, W. Sigmund, J. Magn. Magn. Mater. 322 (2010) 2058.
[16] M. Rasly, M.M. Rashad, J. Magn. Magn. Mater. 337–338 (2013) 58.
[17] M.M. Rashad, A.O. Turky, A.T. Kandil, J. Mater., Sci. Mater. Electron. 24 (2013) 3284.
[18] M.M. Rashad, J. Mater. Sci. Mater. Electron. 23 (2012) 882–888.
[19] D. Bahadur, S. Rajakumar, A. Kumar, J. Chem. Sci. 118 (2006) 15.
[20] B. Ramesh, S. Ramesh, R. Vijaya Kumar, M. Lakshmipathi Rao, J. Alloys Compd. 513 (2012) 289.
[21] A.A. Kadam, S.S. Shinde, S.P. Yadav, P.S. Patil, K.Y. Rajpure, J. Magn. Magn. Mater. 329 (2013) 59.
[22] A.M. Abo El Ata, M.K. El Nimr, S.M. Attia, D. El Kony, A.H. Al-Hammadi, J. Magn. Magn. Mater. 297 (2006) 33.
[23] M. George, S.S. Nair, A.M. John, P.A. Joy, M.R. Anantharaman, J. Phys. D: Appl. Phys. 39 (2006) 900.
[24] M.A. Dar, K.M. Batoo, V. Verma, W.A. Siddiqui, R.K. Kotnala, J Alloys Compd. 493 (2010) 553.
[25] R. Cheruku, G. Govindaraj, L. Vijayan, Mater. Chem. Phys. 146 (2014) 389.
[26] S. Singhal, T. Namgyal, S. Jauhar, N. Lakshmi, S. Bansal, J. Sol–Gel Sci. Technol. 66 (2013) 155.